

Impact of the Crystallinity on the Physical Properties of Inulin during Water Sorption

Sébastien N. Ronkart · Michel Paquot ·
Christophe S. Blecker · Christian Fournies ·
Lynn Doran · Jean Christophe Lambrechts ·
Bernadette Norberg · Claude Deroanne

Received: 29 May 2008 / Accepted: 22 October 2008 / Published online: 1 November 2008
© Springer Science + Business Media, LLC 2008

Abstract The impact of the crystallinity of spray-dried inulins on their stability and physical properties was investigated after a conditioning of 1 week at different relative humidity levels (0% to 94%) at 20 °C. An environmental scanning electron microscopy study showed that the amorphous powders hardened at a relative humidity storage between 59% and 75%; while their semi-crystalline counterparts were partially agglomerated but friable in the

same conditions. Caking was observed when the glass transition temperature of the amorphous phase of the material dropped below the storage temperature of the powder. It resulted in a crystallization of the structural units of varying lengths composing inulin, but also an increase of the crystallinity of the semi-crystalline ones. This study showed the importance of the crystallinity of inulin on its stability and physical properties during storage which is of crucial importance for the shelf-life of food and pharmaceutical products in the dry state.

Financial support was provided for this study by the Walloon Region of Belgium (DGTRE) and Cosucra Groupe Warcoing SA.

S. N. Ronkart (✉) · C. S. Blecker · L. Doran · C. Deroanne
Department of Food Technology,
Gembloux Agricultural University,
Passage des Déportés, 2,
B-5030 Gembloux, Belgium
e-mail: ronkart.s@fsagx.ac.be

S. N. Ronkart · M. Paquot · L. Doran
Department of Industrial Biological Chemistry,
Gembloux Agricultural University,
Passage des Déportés, 2,
B-5030 Gembloux, Belgium

C. Fournies
Cosucra Groupe Warcoing S.A.,
Rue de la Sucrierie, 1,
B-7740 Warcoing, Belgium

J. C. Lambrechts
CERTECH, Analytical Sciences—Microscopy,
Rue Jules Bordet, 1,
B-7180 Seneffe, Belgium

B. Norberg
Department of Structural Biological Chemistry,
The University Faculties of Notre Dame de la Paix,
Rue de Bruxelles, 61,
B-5000 Namur, Belgium

Keywords Inulin · Glass transition · Water sorption · Caking

Introduction

Inulin is a dietary fiber composed of a mixture of oligo- and/or polysaccharides composed of fructose unit chains (linked by (2→1)- β -D-fructosyl-fructose bonds) of various length, terminated generally by a single glucose unit (linked by an α -D-glucopyranosyl bond)^{1,2}.

For now, commercial inulin is mainly extracted from chicory root and is available as a spray-dried powder product. It is well-established that the knowledge of the amorphous fraction of a powder is crucial for predicting its stability during storage^{3,4}. A relatively large amount of works reported the caking of amorphous products exposed to various water vapor pressures^{5,6}. The effects of water content on the solid-state properties of various inulins have been discussed^{7–9}. Schaller-Povolny et al. (2000) pointed out the impact of the molecular weight on the stability of the powder; inulins with higher average degrees of polymerization were more stable than the lower ones⁷. Caking phenomena of amorphous inulins occurred when the glass transition temperature of inulin dropped below the storage temperature. Although

Table 1 Inulin chemical composition of 40/120, 40/230, 95/120 and 95/230

	T_{feed} (°C)				<i>p</i> value
	40		95		
	T_{inlet}				
	120	230	120	230	
Glucose	0.1±0.0	0.1±0.0	0.1±0.0	0.1±0.0	0.239
Fructose	0.4±0.1	0.4±0.0	0.4±0.0	0.4±0.0	0.426
Sucrose	0.4±0.0	0.4±0.0	0.4±0.0	0.4±0.0	0.470
DP 1–10	3.9±0.1	4.0±0.2	3.9±0.2	3.9±0.1	0.822
DP 11–20	24.0±0.6	23.8±0.3	23.7±0.1	23.5±0.4	0.555
DP 21–30	36.5±0.8	37.0±0.3	36.7±0.3	36.2±0.1	0.312
DP 31–40	22.9±0.3	22.9±0.1	22.9±0.1	22.8±0.2	0.861
DP 41–50	8.2±0.3	8.1±0.1	8.3±0.1	8.5±0.1	0.217
DP 51–60	3.0±0.2	2.9±0.1	3.0±0.1	3.3±0.1	0.092
DP>60	1.4±0.2	1.2±0.3	1.4±0.2	1.8±0.2	0.092
DP _n	19.5±0.5	19.5±0.1	19.7±0.3	19.9±0.1	0.140
DP _w	27.6±0.3	27.5±0.2	27.7±0.2	28.0±0.2	0.397

The quantification of glucose, fructose, sucrose, the different DP ranges, DP_n and DP_w has been determined by HPAEC-PAD analysis. Each sample has been spray-dried in triplicate, and the powders have been analyzed in triplicate by HPAEC-PAD. A two-way analysis of variance showed no difference between the samples, as *p* value>0.05 for each constituent

these works have been realized on inulin in an amorphous state, commercial inulins can be either amorphous or semi-crystalline. The crystallinity of the product should also have an impact on the flowability of the powder during storage (i.e., caking). Indeed, it was reported that the degree of crystallinity of microcrystalline cellulose had a significant effect on the stability of formulation in the pharmaceutical domain and it was established that water is sorbed almost exclusively by the amorphous regions of microcrystalline cellulose^{10,11}. Mihranyan et al. (2004)¹² reported that the uptake of water in cellulose powders was notably dependent on the crystallinity content of the product. However, in order to produce celluloses covering a broad range of crystallinity, they prepared them from different sources leading to different chemical compositions. By doing this, we suppose they probably also observed an impact of the molecular weight as well as other physical properties like specific area or porosity, due to the various modes of crystallization used.

For this reason, the aim of this paper was to report the influence of the crystallinity on the physical and flowability properties of inulin powders stored at various water vapor partial pressures. For this purpose, we have used selected pilot spray-dried inulins of identical chemical composition (in glucose, fructose, sucrose, the different degree of polymerization range and the average degree of polymerization in number and in weight), but covering a broad range of crystallinity. The resulting glass transition temperature (T_g) and crystallinity of inulins were determined by modulated differential-scanning calorimetry (MDSC) and wide-angle X-ray scattering (WAXS), respectively. In

addition, the inter-particle properties which were related to the powder stability were visualized by environmental scanning electron microscopy (ESEM).

Materials and Methods

Materials

Fibruline® XL (Cosucra Groupe Warcoing SA, Warcoing, Belgium) was dispersed in distilled water (to a solid

Table 2 Water content (g water/100 g dry inulin) experimental values± standard deviation of 40/120, 40/230, 95/120, and 95/230 stored one week at various relative humidities at 20 °C (*n*=4)

RH	FT			
	40		95	
	T_{inlet}			
	120	230	120	230
0	0.6±0.1	0.7±0.2	0.5±0.1	0.9±0.4
12	6.5±0.6	5.4±0.1	4.7±0.4	4.4±0.0
33	8.5±0.1	7.8±0.0	8.2±0.2	7.3±0.5
59	11.9±0.7	11.9±0.4	12.3±0.1	11.4±2.1
75	14.2±0.1	13.9±0.1	15.0±0.2	14.7±0.6
94	20.8±0.5	19.8±0.9	19.2±0.1	19.0±0.9

FT feed temperature (°C), T_{inlet} inlet air temperature of the spray drier (°C), RH relative humidity (%)

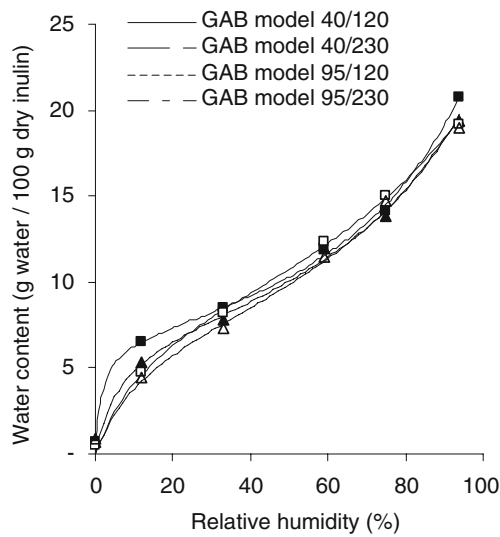
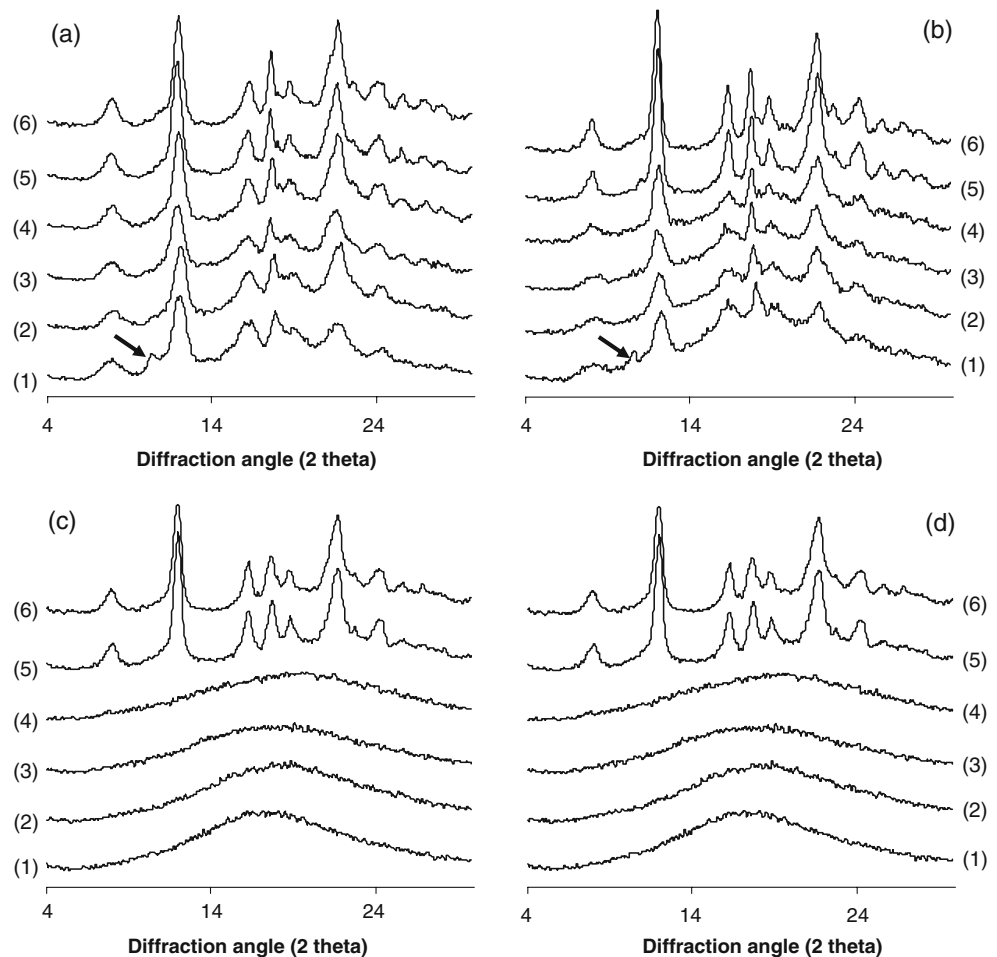


Fig. 1 Sorption isotherms at 20 °C of 40/120, 40/230, 95/120 and 95/230 at six relative humidities storage (0, 12, 33, 59, 75, and 94%). The GAB model has been fitted to each set of experimental values. (filled square) 40/120 (^aFT, 40 °C, ^bT_{inlet}, 120 °C); (filled upright triangle) 40/230 (^aFT, 40 °C, ^bT_{inlet}, 230 °C); (empty square) 95/120 (^aFT, 95 °C, ^bT_{inlet}, 120 °C); and (empty upright triangle) 95/230 (^aFT, 95 °C, ^bT_{inlet}, 230 °C). ^aFeed temperature (°C). ^bInlet air temperature of the spray drier (°C)

concentration of 20%, w/w) at 40 or 95 °C, then spray-dried in a pilot plant scale Anhydro Lab S1 spray drier (Anhydro, Denmark) with an inlet air temperature of 120 or 230 °C¹³. The resulting powders were labeled 40/120, 40/230, 95/120, and 95/230, referring to the feed temperature (40 and 95 °C) and to the inlet air temperature of the spray drier (120 and 230 °C). The chemical composition of inulins is presented in Table 1 and was determined by High Performance Anion Exchange Chromatography coupled with a Pulsed Amperometric Detector (HPAEC-PAD) using a procedure detailed in Ronkart et al. (2007)¹⁴. All samples presented the same content in glucose, fructose, sucrose, the different degree of polymerization range and the average degree of polymerization in number (DP_n) and in weight (DP_w). Inulins were initially dried over P₂O₅ (one week), then conditioned one week at 20 °C at different relative humidities by storing them in desiccators containing different saturated salt solutions (P₂O₅, LiCl, MgCl₂, NaBr, NaCl and KNO₃). These salts covered a large relative humidity range (~0–94% at 20 °C).

Fig. 2 Wide-angle X-ray scattering diffractograms of amorphous and semi-crystalline inulins obtained on sorption isotherm in the relative humidity range (~0–94% at 20 °C). The different relative humidity used were (1) 0, (2) 12, (3) 33, (4) 59, (5) 75 and (6) 94%. **a** 40/120 (^aFT, 40 °C, ^bT_{inlet}, 120 °C); **b** 40/230 (^aFT, 40 °C, ^bT_{inlet}, 230 °C); **c** 95/120 (^aFT, 95 °C, ^bT_{inlet}, 120 °C) and **d** 95/230 (^aFT, 95 °C, ^bT_{inlet}, 230 °C). ^aFT Feed temperature (°C). ^bT_{inlet} inlet air temperature of the spray drier (°C)



Water Content by Volumetric Karl Fischer Titration

The total water content of inulin was determined by a Karl Fischer titrator DL31 from Mettler Toledo using Hydranal® methanol rapid and the one-component reagent for volumetric Karl Fischer titration Hydranal® composite 5 (5 mg H₂O ml⁻¹), both purchased from Riedel-de Haën (Seelze, Germany). The methodology used and the experimental precautions are fully described in Ronkart et al. (2006)¹⁵.

Wide-angle X-ray Scattering (WAXS)

The apparatus used was a PW3710 Philips Analytical X-ray B.V. with a Ni-filtered CuK_α radiation ($\lambda=1.54178$ Å), generated by an anode device operating at 40 kV and 30 mA in conjunction with a proportional detector. The patterns were recorded with a fixed time of 0.4 s per step of 0.02° in the 4° < 2θ < 30° range, at 20 °C.

Modulated Differential-scanning Calorimetry (MDSC)

The thermal properties of powders were examined with a 2920 TA Instruments (New Castle, DE) with a refrigerated cooling accessory and modulated capability. The cell was purged with 70 ml min⁻¹ dry nitrogen, calibrated for baseline on an empty oven and for temperature using two temperature standards (indium T_{onset} , 156.6 °C; eicosane T_{onset} , 36.8 °C). Specific heat capacity (C_p) was calibrated using a sapphire. The empty sample and reference pans were of equal mass to within ±0.10 mg. The sample mass was precisely weighed and was around 7 mg. All measurements were made at least in triplicate. The heating rate was 1.5 °C min⁻¹, while the amplitude and the period of the MDSC were 1.5 °C and 90 s, respectively.

Thermal profiles were obtained over a temperature range of 20 to 220 °C by using non-hermetic aluminum pans. The experiments allowed the visualization of the water evaporation, dry glass transition, melting, and browning/degradation. The impact of the water content to T_g was investigated in the -50 °C to 200 °C range by using hermetic aluminum pans in order to avoid water loss during the thermal analysis.

Environmental Scanning Electron Microscopy

The particle shape and the surface morphology at the micrometer scale were investigated with an Environmental Scanning Electron Microscope (ESEM), XL30 type ESEM-FEG (Philips/FEI) at 20 kV, using wet mode at 3.3–3.5 torr and a working distance of 10.0 mm. The detection system used was a Gaseous Secondary Electron Detector.

Results and Discussion

Water Sorption

The experimental water content and water activity values of inulins stored 1 week at various relative humidities at 20 °C are given in Table 2. Figure 1 presents the water content of 40/120, 40/230, 95/120, and 95/230 exposed 1 week to a relative humidity comprised between 0% and 94%. The GAB (Guggenheim, Anderson and de Boer) mathematical model was fitted to the experimental data as described in detail elsewhere⁹. In the low RH range (0–12%), the semi-crystalline inulins contained more water than their amorphous counterparts. Indeed, the semi-crystalline inulin 40/120 and its amorphous counterpart 95/120 showed a significant difference in their water content at 12% RH (6.5±0.6 g water/100 g dry inulin and 4.7±0.4 g water/100 g dry inulin for 40/120 and 95/120, respectively); while the intermediate crystalline inulin (40/230) was characterized by an intermediate water content (5.4±0.1 g water/100 g dry inulin).

Development of Crystallinity

Figure 2 shows the crystallinity changes of 40/120, 40/230, 95/120, and 95/230 stored at different relative humidities at 20 °C. Diffractograms in the 4° < 2θ < 30° range presented

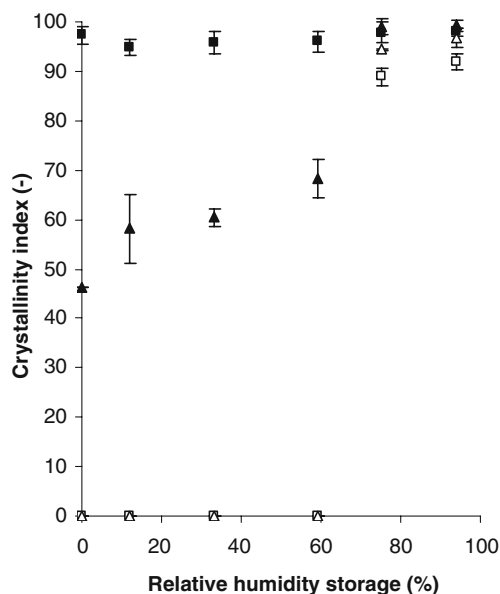


Fig. 3 Evolution of the crystallinity index (in the 4° < 2θ < 30° range) of inulin samples during storage over different saturated salts covering a large range of relative humidity (~0–94%) at 20 °C. (filled square) 40/120 (^aFT, 40 °C, ^bT_{inlet}, 120 °C); (filled upright triangle) 40/230 (^aFT, 40 °C, ^bT_{inlet}, 230 °C); (empty square) 95/120 (^aFT, 95 °C, ^bT_{inlet}, 120 °C); and (empty upright triangle) 95/230 (^aFT, 95 °C, ^bT_{inlet}, 230 °C). ^aFT, feed temperature (°C). ^bT_{inlet}, inlet air temperature of the spray drier (°C)

either a broad halo pattern, or diffraction peaks, characteristic of an amorphous or a semi-crystalline inulin, respectively. The positions and the relative intensity of peaks are very close to those reported by André et al. (1996) on chicory root inulin precipitated by ethanol, and corresponded to two hydration states of the crystals^{16,17}. The main difference between these polymorphs does not correspond to any change in conformation of inulin, but rather to a variation in the number of water molecules in the unit cell. The hemi-hydrate has half a water molecule per fructosyl residue; while the mono-hydrate presents between one half and one water molecule per fructosyl residue. The reflection at $2\theta=10.6^\circ$ (arrow in Figure 2a,b) is the only main difference between the two hydration states and is completely absent in the hydrated state^{1,17}. Such a difference in this diffraction peak has been attributed by André (1995) to a variation in the torsion angle of the hydroxymethyl group due to the hydrogen bonds in the unit cell lattice¹⁸. The WAXS crystallinity indexes (CI) were estimated from the ratio of the integrated intensities of the diffraction peaks to the total integrated intensity of coherent scattering after appropriate baseline subtraction¹⁹. The inulins obtained from spray-drying dispersions at 40 °C

were semi-crystalline, while those at 95 °C were completely amorphous. The spray-drying of the feed at 40 °C with an inlet air temperature of 230 °C (CI=46.3%), led to a more amorphous inulin than its counterpart spray-dried at 120 °C (CI=97.3%), probably due to partial melting of crystals inside the spray drier. The increasing intensities and peak areas showed a clear development of crystallinity (Figure 3) for inulins stored at 75% relative humidity and above. These results confirmed a crystallization, resulting from an increase in the system's mobility (facilitated by water), which favored reordering into a more stable crystalline structure. At RH=94%, the crystallinity index of the initially amorphous inulins (CI of 95/120=91.9% and CI of 95/230=96.7%) were below those of their counterparts 40/120 (CI=97.9%) and 40/230 (CI=99.2%). This difference can be explained by the fact that the crystallization of the whole amorphous matrix could physically entrap an amorphous fraction and this part is too highly constrained to crystallize further. These kinds of results were previously reported by Mizuno et al. (1998) who showed that the crystallization of amorphous starch induced crystals acting as physical cross-links that restricted the mobility of the polymer chains²⁰.

Fig. 4 Modulated differential-scanning calorimetry thermograms of 40/120, 40/230, 95/120, and 95/230 obtained on adsorption isotherm in the relative humidity range (~0–94% at 20 °C). The different relative humidity used were (1) 0, (2) 12, (3) 33, (4) 59, (5) 75, and (6) 94%. **a,b** 40/120 (^aFT, 40 °C, ^b T_{inlet} , 120 °C); **c,d** 40/230 (^aFT, 40 °C, ^b T_{inlet} , 230 °C); **e,f** 95/120 (^aFT, 95 °C, ^b T_{inlet} , 120 °C) and **g,h** 95/230 (^aFT, 95 °C, ^b T_{inlet} , 230 °C). ^aFT, feed temperature (°C). ^b T_{inlet} , inlet air temperature of the spray drier (°C)

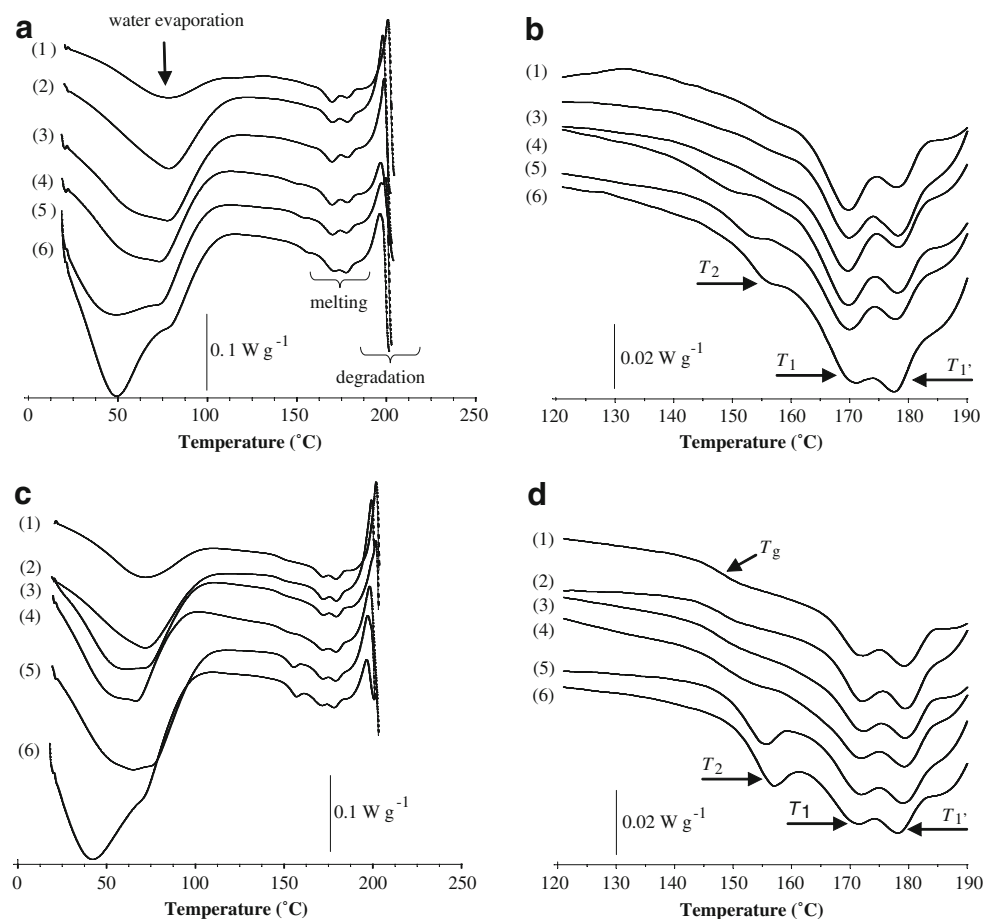
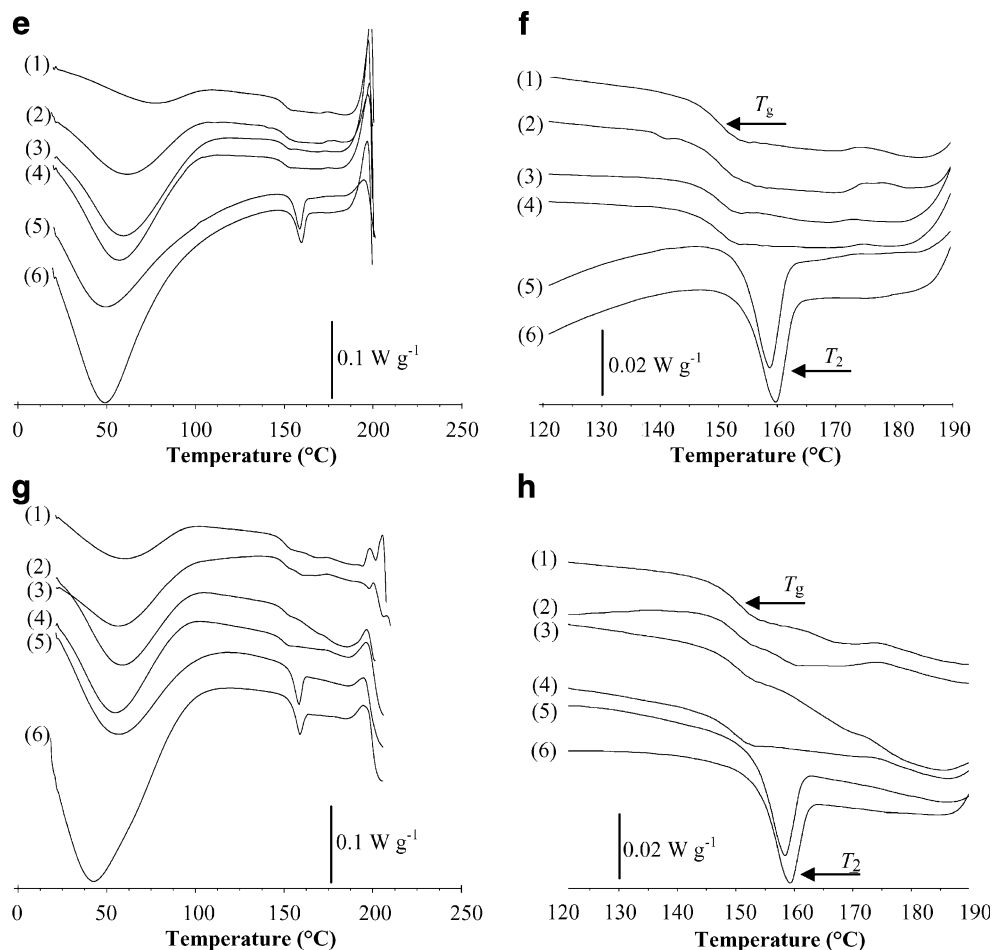


Fig. 4 (continued)



Thermal Properties

Stored at 0–59% RH, the semi-crystalline inulins were characterized by a dual endothermic peak (labeled peak 1 and 1') at $T_1=171\text{--}172\text{ }^\circ\text{C}$ and $T_1'=178\text{--}179\text{ }^\circ\text{C}$, which corresponded to the melting of two populations of crystals which probably differed by their shape, size, perfection, and/or molecular weight and thus led to different thermal properties (Figure 4a,b). The thermal profile (in open pans) of fully amorphous inulins was characterized by a jump at around $150\text{ }^\circ\text{C}$, which corresponded to the glass transition temperature (Figure 4c,d). When the inulins crystallized from the fully amorphous product (at 75% RH and above), an endothermic peak appeared at $T_2=160\text{ }^\circ\text{C}$. In a previous study, we have shown by Temperature-resolved wide-angle X-ray scattering analysis that it was due to the melting of formed crystals at high humidity storage²¹.

Crystallized 40/120 and 40/230 inulins (at 75–94% RH) were characterized by an additional endothermic peak at $T_2=157\text{ }^\circ\text{C}$ probably due to the formation of less perfect crystals than those initially present in the semi-crystalline powder. It resulted in the presence of different crystal

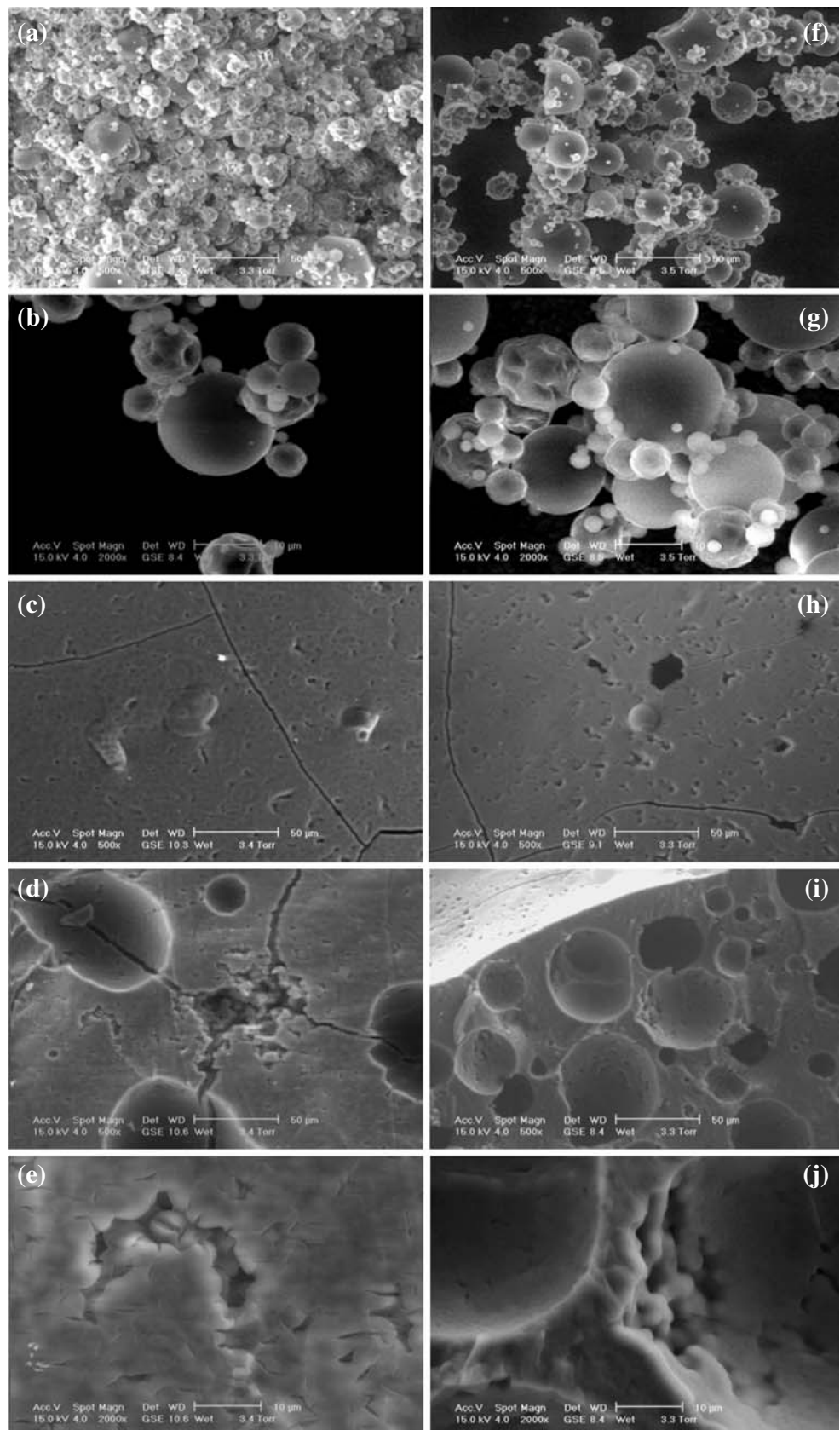
Table 3 Evolution of the glass transition temperature±standard deviation of 40/120, 40/230, 95/120, and 95/230 related to their relative humidity storage (0, 12, 33, 59, 75, and 94% RH at $20\text{ }^\circ\text{C}$)

RH	FT			
	40		95	
	T_{inlet}			
	120	230	120	230
0	138.9±1.8	136.5±2.4	132.6±0.9	143.1±6.3
12	84.1±1.1	84.4±1.4	86.8±0.7	85.8±1.6
33	58.6±1.8	60.9±0.9	60.3±0.4	64.5±2.5
59	31.7±2.4	29.1±0.7	30.5±1.1	31.7±2.4
75	17.9±0.2	–	–	–
94	–	–	–	–

(a) FT, $40\text{ }^\circ\text{C}$, T_{inlet} , $120\text{ }^\circ\text{C}$; (b) FT, $40\text{ }^\circ\text{C}$, T_{inlet} , $230\text{ }^\circ\text{C}$; (c) FT, $95\text{ }^\circ\text{C}$, T_{inlet} , $120\text{ }^\circ\text{C}$ and (d) FT, $95\text{ }^\circ\text{C}$, T_{inlet} , $230\text{ }^\circ\text{C}$

FT feed temperature ($^\circ\text{C}$), T_{inlet} inlet air temperature of the spray drier ($^\circ\text{C}$), RH relative humidity (%)

Fig. 5 ESEM micrographs of inulin dispersed at 95 °C then spray-dried with an inlet air temperature of 120 (a–e) or 230 °C (f–j). 95/120 stored 1 week at (a–b) 0 or (c–e) 94% RH; 95/230 stored 1 week at (f–g) 0 or (h–j) 94% RH. Scale bar for a, c, d, f, h, and i, 50 μm; scale bar for b, e, g, and j, 10 μm



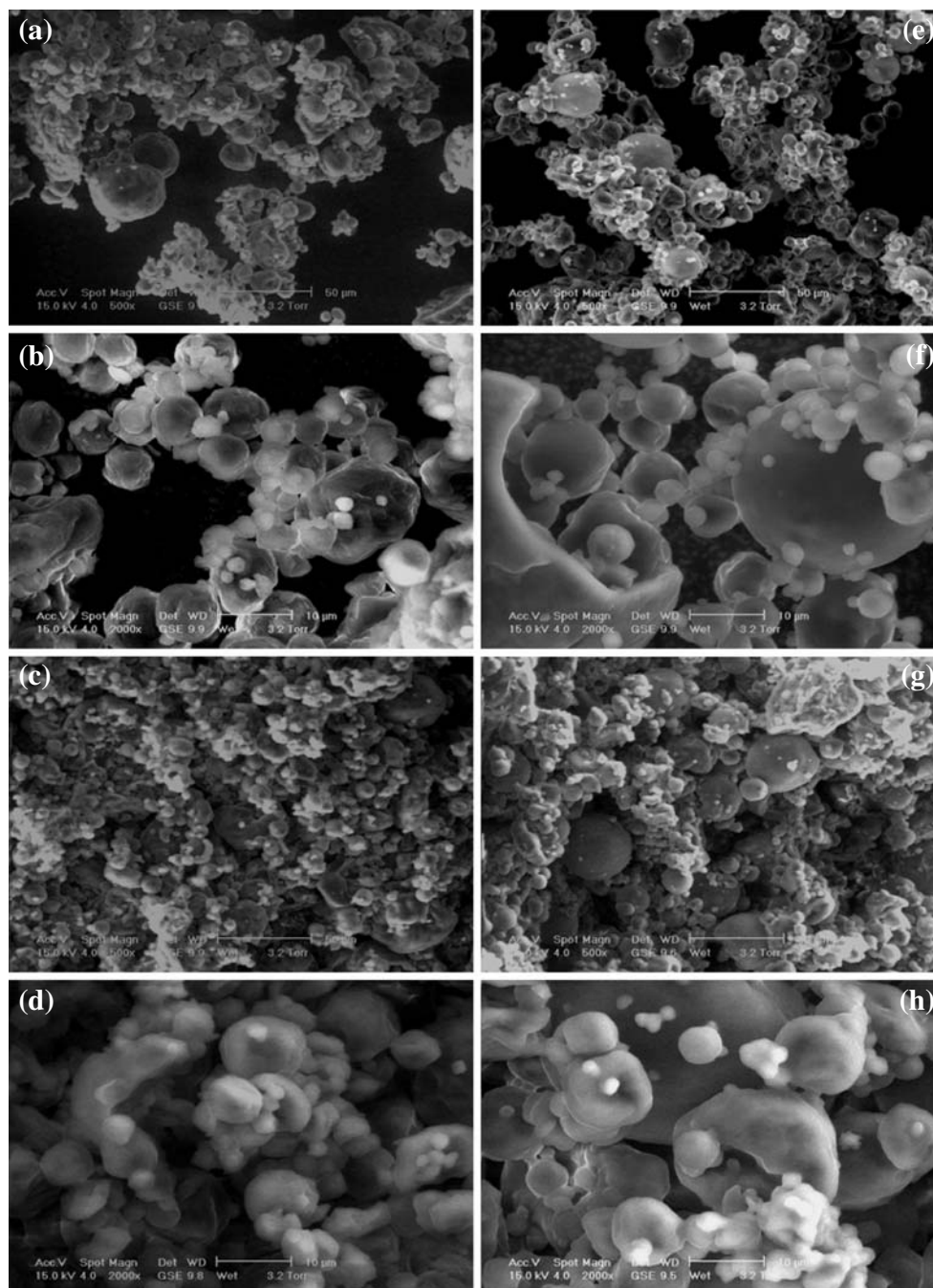
populations which differed by their thermal stability and thus their thermal profile. Peak 2 was more pronounced for 40/230 than 40/120, as the amorphous fraction was more important and thus led to a higher capacity to crystallize.

Glass Transition Temperature

The impact of the sorbed water on the T_g of amorphous and semi-crystalline inulins was investigated (Table 3). For this purpose, aluminum hermetic pans were used for the MDSC experiments to avoid water evaporation during thermal

analysis. So, the determined T_g were not from the thermograms obtained by using non-hermetic pans as shown in Figure 4. All inulins (including the semi-crystalline ones) were characterized by an amorphous fraction, and thus a T_g . By its plasticizing effect on inulin, the increase of the water content decreased the T_g of the samples^{7–9}. As soon as this transition dropped below storage temperature (20 °C), stability and physical properties of inulins changed. Crystallization due to an increased mobility of the molecules in the sample has been reported on many biomacromolecules²² and usually leads to flowing or stability

Fig. 6 ESEM micrographs of inulin dispersed at 40 °C then spray-dried with an inlet air temperature of 120 (a–d) or 230 °C (e–h). 40/120 stored 1 week at (a, b) 0 or (c, d) 94% RH; 40/230 stored 1 week at (e, f) 0 or (g, h) 94% RH. Scale bar for a, c, e, and g, 50 μ m; scale bar for b, d, f, and h, 10 μ m



problems of the powder, i.e., caking. In this study, crystallization occurred at $T_g < 20$ °C and no glass transition was observable in crystallized inulins. However, it was supposed that the material presented an amorphous fraction and the associated glass transition was superimposed to the melting of the crystals because a difference in the heat capacity between the onset and endset of the melting peak was observed in the thermal profile.

Stability of the Powder

ESEM micrographs of inulins stored 1 week at 0% RH (Figure 5a,b,f,g and Figure 6a,b,e,f) showed products in a powder form. As reported in a previous paper on spray-dried inulin, an inlet air temperature (T_{in}) of 230 °C led to a blow-out of some of the particles; while those spray-dried at $T_{in} = 120$ °C were intact¹³. Moreover, samples 40/120 and 40/230 presented a rough surface; while the amorphous ones (95/120 and 95/230) were smooth. This difference was due to the properties of the feed before the spray-drying. Indeed, suspended particles in the feed led to powders with rough surfaces; while the spray-drying of a solution rather than a suspension provided particles with a smooth surface.

Water is sorbed on the dry particles from the conditioned atmospheres. The powders caked as the glass transition fell below 20 °C, at a storage humidity between 59 and 75% (Table 3). The viscosity drop of the material led to inter-particles fusion, and thus the caking of the powder which could be anything from small soft aggregates that broke easily to solidification of the whole powder mass²³. The flowability loss of the product changed depending on the initial crystallinity of inulin.

Samples 40/120 and 40/230 stored 1 week at 59–94% RH were slightly agglomerated but the entire product was easily friable (Figure 6c–d, g–h). This state has been characterized by Ruan et al. (2007) as bridging and is the initial stage of caking occurring as a result of the sticky contact points between particles²³. In this state, small inter-particle bridges may be disintegrated under mild shaking. The formation of a continuous mass was observed for the initial amorphous samples (95/120 and 95/230) stored at 75–94% RH (Figure 5c,h). In these conditions, the particles appeared fused-agglomerated (Figure 5d,e,i,j). The hardening of these inulins can be explained by the crystallization of the entire amorphous product, as confirmed by the diffractograms presented in Figure 2. Tight and orderly molecular packing during crystallization cannot generally accommodate excess water which results in the loss of adsorbed water and absorption of this ejected water at the surface of neighboring particles. This results in inter-particle liquid bridges leading to caking²⁴. This mechanism known as humidity caking is typical for powders that are water-soluble or contain water-soluble materials²³. In the

case of 40/120 and 40/230, we have shown that the presence of crystals in the amorphous matrix limited the advanced caking of inulins.

Conclusions

This study pointed out the importance of inulin crystallinity in regards to its behavior during humidity storage. Amorphous inulins hardened at RH > 75%; while their semi-crystalline counterparts were agglomerated but friable in the same humidity conditions. These caking phenomena occurred as the T_g dropped below storage temperature (20 °C). This resulted in a crystallization of the amorphous fraction for both amorphous and semi-crystalline inulins, leading to a melting peak in the MDSC thermograms around the glass transition. In the low humidity range, the semi-crystalline inulins were more hygroscopic than their amorphous counterpart, which is in contradiction with the general thinking that amorphous materials are more hygroscopic than crystalline ones. The difference in the stability between the semi-crystalline inulins and their amorphous counterparts is of crucial importance for the behavior of inulin during process, storage or incorporation in high moisture formulations. This study will help to predict the solid-state behavior of inulin powders in regards to humidity. It could also be extended to other molecules presenting similar properties, such as the presence of an amorphous phase or polymorphic transitions.

Acknowledgment The authors are grateful to Prof Johan Wouters from the ‘Department of Structural Biological Chemistry’ of the ‘The University Faculties of Notre Dame de la Paix’ (Namur, Belgium) for the X-ray facilities.

References

1. R.H. Marchessault, T. Bleha, Y. Deslandes, J.-F. Revol, *Can. J. Chem* **58**, 2415 (1980). doi:10.1139/v80-390
2. M.B. Roberfroid, N.M. Delzenne, *Annu. Rev. Nutr* **18**, 117 (1998). doi:10.1146/annurev.nutr.18.1.117
3. B.R. Bhandari, T. Howes, *J. Food. Eng* **40**, 71 (1999). doi:10.1016/S0260-8774(99)00039-4
4. J.M. Aguilera, J.M. del Valle, M. Karel, *Trends Food Sci. Technol* **6**, 149 (1995). doi:10.1016/S0924-2244(00)89023-8
5. M. Le Meste, D. Champion, G. Roudaut, G. Blond, D. Simatos, *J. Food Sci* **67**, 2444 (2002). doi:10.1111/j.1365-2621.2002.tb08758.x
6. R.J. Lloyd, X.D. Chen, J.B. Hargreaves, *Int. J. Food Sci. Technol* **31**, 305 (1996). doi:10.1046/j.1365-2621.1996.00352.x
7. L.A. Schaller-Povolny, D.E. Smith, T.P. Labuza, *Int. J. Food Prop* **3**, 173 (2000)
8. J.E. Zimeri, J.L. Kokini, *Carbohydr. Polym* **48**, 299 (2002). doi:10.1016/S0144-8617(01)00260-0

9. S. Ronkart, C. Blecker, C. Fougnyes, J.-C. Van Herck, J. Wouters, M. Paquot, *Carbohydr. Polym* **63**, 210 (2006). doi:[10.1016/j.carbpol.2005.08.030](https://doi.org/10.1016/j.carbpol.2005.08.030)
10. Airaksinen S PhD. Thesis, 2005, Division of Pharmaceutical Technology, Faculty of Pharmacy, University of Helsinki (Finland)
11. S. Airaksinen, M. Karjalainen, A. Shevchenko et al., *J. Pharm. Sci.-US* **94**, 2147 (2005)
12. A. Mhranyan, A.P. Llagostera, R. Karmhag, M. Strømme, R. Ek, *Int. J. Pharm* **269**, 433 (2004). doi:[10.1016/j.ijpharm.2003.09.030](https://doi.org/10.1016/j.ijpharm.2003.09.030)
13. S.N. Ronkart, C. Deroanne, M. Paquot, C. Fougnyes, J.-C. Lambrechts, C. Blecker, *Food Biophys* **2**, 83 (2007). doi:[10.1007/s11483-007-9034-7](https://doi.org/10.1007/s11483-007-9034-7)
14. S.N. Ronkart, C. Blecker, H. Fourmanoir et al., *Anal. Chim. Acta* **604**, 81 (2007). doi:[10.1016/j.aca.2007.07.073](https://doi.org/10.1016/j.aca.2007.07.073)
15. S.N. Ronkart, M. Paquot, C. Fougnyes, C. Deroanne, J.-C. Van Herck, C. Blecker, *Talanta* **70**, 1006 (2006). doi:[10.1016/j.talanta.2006.02.024](https://doi.org/10.1016/j.talanta.2006.02.024)
16. I André, K. Mazeau, I. Tvaroska et al., *Macromolecules* **29**, 4626 (1996). doi:[10.1021/ma951799f](https://doi.org/10.1021/ma951799f)
17. I. André, J.L. Putaux, H. Chanzy, F.R. Tavel, J.W. Timmermans, D. de Wit, *Int. J. Biol. Macromol* **18**, 195 (1996). doi:[10.1016/0141-8130\(95\)01075-0](https://doi.org/10.1016/0141-8130(95)01075-0)
18. I. André. Etudes structurales et dynamiques de l'inuline et de sophoranes cycliques et linéaires. 1995, PhD Thesis, Université Joseph Fourier, France
19. H. Xu, B. Seyhan Ince, P. Cebe, *J. Polym. Sci. Pol. Phys* **41**, 3026 (2003). doi:[10.1002/polb.10625](https://doi.org/10.1002/polb.10625)
20. A. Mizuno, M. Mitsuiki, M. Motoki, *J. Agric. Food Chem* **46**, 98 (1998). doi:[10.1021/jf970612b](https://doi.org/10.1021/jf970612b)
21. S.N. Ronkart, M. Paquot, C. Fougnyes, C. Deroanne, C.S. Blecker, *Food Hydrocolloid* **23**, 922 (2009). doi:[10.1016/j.foodhyd.2008.06.003](https://doi.org/10.1016/j.foodhyd.2008.06.003)
22. A.P. Mathew, A. Dufresne, *Biomacromolecules* **3**, 1101 (2002). doi:[10.1021/bm020065p](https://doi.org/10.1021/bm020065p)
23. R. Ruan, Y.-J. Choi, M.-S. Chung, *Food Sci. Biotechnol* **16**, 329 (2007)
24. M. Saltmarch, T.P. Labuza, *J. Food Sci* **45**, 1231 (1980). doi:[10.1111/j.1365-2621.1980.tb06528.x](https://doi.org/10.1111/j.1365-2621.1980.tb06528.x)